STUDY OF FATIGUE CRACK PROPAGATION RATE IN ALUMINIUM AND MILD STEEL

By

RAVINDER KUMAR SEHGAL

DEPARTMENT OF MECHANICAL ENGINEERING

INDIAN INSTITUTE OF TECHNOLOGY KANPUR

FEBRUARY 1974

STUDY OF FATIGUE CRACK PROPAGATION RATE IN ALUMINIUM AND MILD STEEL

A Thesis Submitted
In Partial Fulfilment of the Requirements
for the Degree of
MASTER OF TECHNOLOGY

By

RAVINDER KUMAR SEHGAL

to the

DEPARTMENT OF MECHANICAL ENGINEERING
INDIAN INSTITUTE OF TECHNOLOGY KANPUR

FEBRUARY 1974

CERTIFICATE

This is to certify that this work on "Study of Fatigue-Crack Propagation Rate in Aluminium and Mild Steel" has been carried out under my supervision, and has not been submitted elsewhere for a degree.

February 3, 1974

S. N. Bandyopadhyay

Dr. S.N. Bandyopadhyay
Assistant Professor
Department of Mechanical Engg.
Indian Institute of Technology
Kanpur-208016, India

ACKNOWLEDGEMENTS

I am extremely indebted to Dr. S.N. Bandyopadhyay for his constant inspiration and invaluable guidance throughout the course of present work.

I am extremely thankful to Mr. Abdul Mubeen for his help in performing experiments, and for useful discussions and suggestions during the experimentation.

I would like to thank Mr. Rahman of Material Testing Lab. for his kind co-operation and all other friends for their kind assistance throughout the work.

Ravinder Kumar Sehgal

LIST OF CONTENTS

CHAPTER

***

LIST OF FIGURES

* * *

NOMENCLATURE

n	Number of fatigue cycles
a_o	Half crack length before fatigue loading, mms
a	Fatigue half crack length, mms.
σ	Range of stress, Kg/mm^2
σ_{max}	Maximum Tensile stress, Kg/mm^2
σ_{min}	Minimum tensile stress, Kg/mm^2
σ_a	Applied stress, Kg/mm^2
P_{max}	Maximum tensile load, Kg.
P_{min}	Minimum tensile load, Kg.
K_{max}	Maximum stress intensity factor, $Kg/mm^2\sqrt{mm}$
K_{min}	Minimum stress intensity, factor $(Kg/mm^2)\sqrt{mm}$
ΔK	Range of stress intensity factor $(Kg/mm^2)\sqrt{mm}$
p	Plastic zone size, mms.
ρ	Radius of curvature at the crack tip, mms.
$\bar{U}$	Rate of external work
$\bar{V}$	Rate of elastic energy
$\bar{T}$	Rate of kinetic energy
$\bar{E}_c$	Rate of crack closure energy
$\bar{D}$	Rate of energy dissipation
C_1, C_2, C_3, C_4	Material constants
m	Index of power law
$\frac{da}{dn}$	Crack propagation rate mms/cycle

ABSTRACT

An experimental investigation of fatigue-crack growth rate at low strain rate in aluminium and mild steel has been presented. Crack-propagation laws are established for these materials at low strain-rate cycling under room temperature conditions. The tests were conducted in thin sheet - centre cracked specimens designed as per ASTM - S.T.P. 410 specifications.

The difference between the maximum and minimum stress intensity factors for a crack ($\Delta K = K_{max} - K_{min}$) has been varied as the crack propagates under fatigue loading. For aluminium the ΔK was studied in the range 8.85 to 23.16 Kg/$mm^2\sqrt{mm}$ whereas in the case of mild steel the range was 15.00 to 35.00 Kg/$mm^2\sqrt{mm}$.

It was found that the rate of fatigue-crack propagation is proportional to $(\Delta K)^m$ where m is a constant dependent on the range of ΔK. Furthermore it was observed that the value of m altered at a particular value of ΔK.

The crack toughness values for aluminium and mild steel are also reported.

* * *

CHAPTER I

INTRODUCTION

1.1 Metal Fatigue:

The phenomenon of the structural failure by catastophic crack propagation at average stresses well below the yield strength has been observed for many years. Recent developments of various new materials and the broadening range of their application particularly in defence, aerospace and cryogenic industries have given considerable emphasis on the problem of fatigue-fracture failures.

Machine and structural members are often subjected to loads that do not remain constant but vary with time. These failures occurring under the condition of dynamic loading are called fatigue failures. The process of fatigue failure can be described in three different phases namely, the nucleation of the micro-cracks, propagation phase of the fatigue cracks and final fracture-failure of the material. However, the distinction between the first two phases is not very clear. The nucleation phase is primarily related to the micro-structure and surface conditions of the material while the term "fatigue crack propagation" is generally used for the growth of micro-cracks. If the machine component under the fatigue loading is rather bulky with no distinct stress raiser, the nucleation period of the fatigue crack would be very long, compared to the propagation period. In such cases, the techniques used

for the prediction of fatigue life are based on the studies leading to S-N-type curves. On the other hand, in structures with severe stress concentrations like notches, particularly in thin plates and shells, the formation of a dominant macrocrack takes place relatively early in the fatigue life, and, hence, in terms of the number of load cycles, the propagation phase constitutes the major portion of the total life.

As the material undergoes repeated cyclic stresses it becomes softer due to the process of work-softening at some strain concentrating features as a notch and alternating slip can occur in a few slip bands. This repetition of slip in the same region allows small increments of microcrack failures which might be insignificant in a single stress cycle. The slip bands produce slip steps on the free surface of the material which gradually become deep ridges and grooves. These grooves, grow into the material as "intrusions" along the slip bands and a few of the deep ones eventually develop as fatigue crack. Once a particular deep groove has formed, the strain or stress concentrating action of its tip helps it to grow and propagate deeply down its slip planes and ultimately cause the fatigue fracture.

1.2 Crack Initiation and its Propagation:

The development and propagation of fatigue crack takes place in two stages.

First stage, illustrated in Fig. 1.1, is characterized

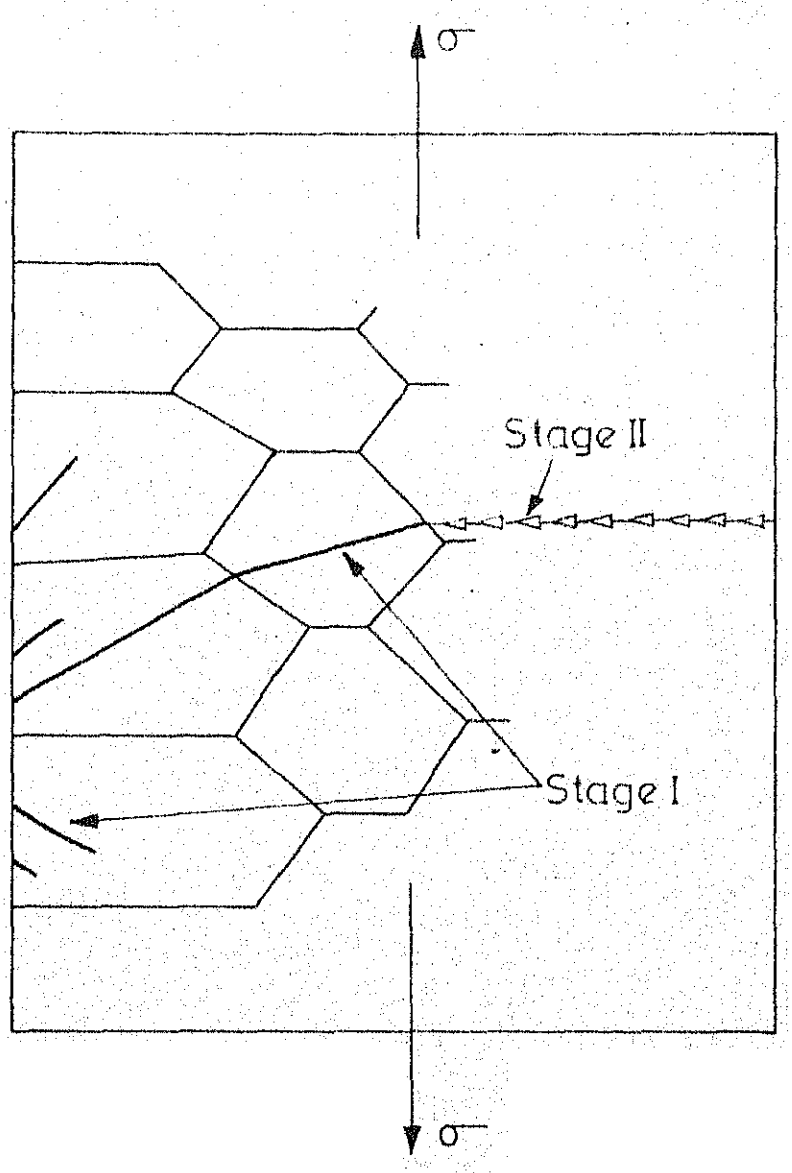

Fig. 1.1 - Schematic representation of the two stage crack propagation.

by propagation of the crack on a plane oriented at approximately 45° to the stress axis while the second stage propagated at 90° to the stress axis and the fracture surface is covered by striations running parallel to the crack propagation front.

In high strain fatigue, failure takes place predominantly by stage-II crack propagation since, the crack propagation rate in stage-II growth can reach values of microns per cycle, the phenomena associated with the growth mechanism are fairly large and easy to observe. Direct observation of the changes occurring at crack tips under cyclic loads indicate that a crack propagates by plastic blunting of the crack tip during the tensile part of the fatigue cycle followed by resharpening of the crack in the compression part. This process of crack growth is called "Plastic Blunting Process" and is illustrated in Fig. 1.2.

1.3 Crack Propagation Mechanism in Pulsating Tension:

The present work is on the study of crack propagation rate under pulsating tensile loading. Resharpening of the crack in the compression part of the fatigue cycle is an essential component of the plastic blunting process. However, fracture surface striations are generally observed in ductile materials like aluminium broken in pulsating tension tests on sheet specimens. Any ductile metal subjected to pulsating tension test will work-harden rapidly to saturation hardness

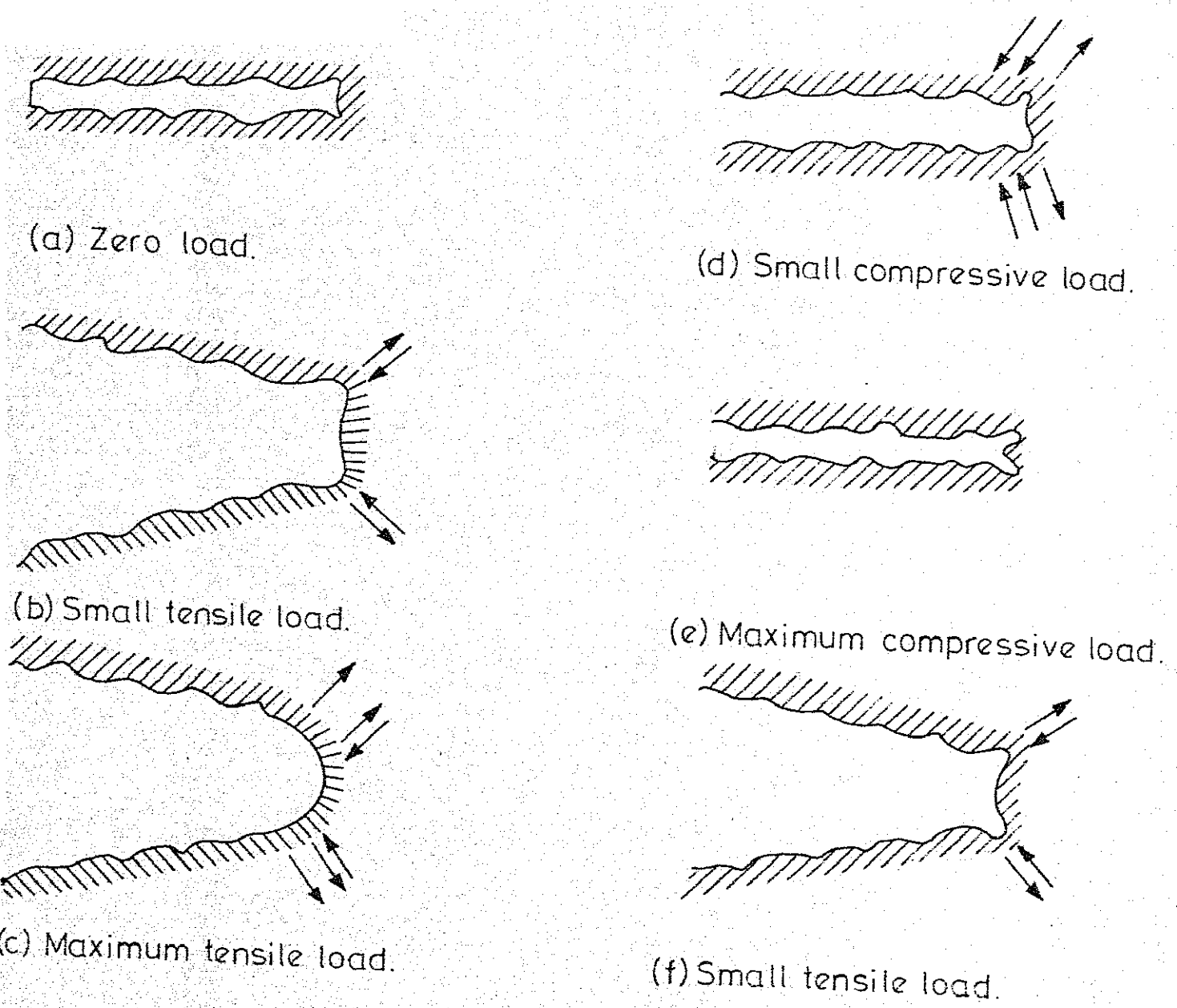

Fig.1.2 - The plastic blunting process of fatigue crack propagation in the stage II mode.

even at stresses upto the ultimate tensile strength. The pulsating stress strain loop will, therefore, quickly attain equilibrium as shown in Fig. 1.3 and in this form will be a closed very narrow loop. Any small degree of localized plastic deformation occurring at a crack tip will be reversed by the total elastic constraint of the specimen as the applied stress falls to zero. Even a small decrease of stress from the maximum applied tensile stress of the cycle will cause a local reversal of strain at a crack tip, an associated crack tip fold and, therefore, a fracture surface straition.

1.4 Stage-II Crack Propagation in Thin Sheet Specimens:

Cracks propagating by stage-II mode in thin sheets frequently change their plane of propagation from one at 90° to the stress axis to another which is at 45° both to the stress axis and the plane of the sheet. This generally occurs when the crack is long and when the plastic zone at the crack tip is accordingly of large size. In this situation slip bands begin to operate at 45° to the plane of the sheet. The plastic blunting process thus becomes one of "slipping off" by plastic deformation in combination with the rounding off process. Striations formed in such cases are not so well pronounced and in some cases are completely obliterated by the rubbing together of the fracture surfaces.

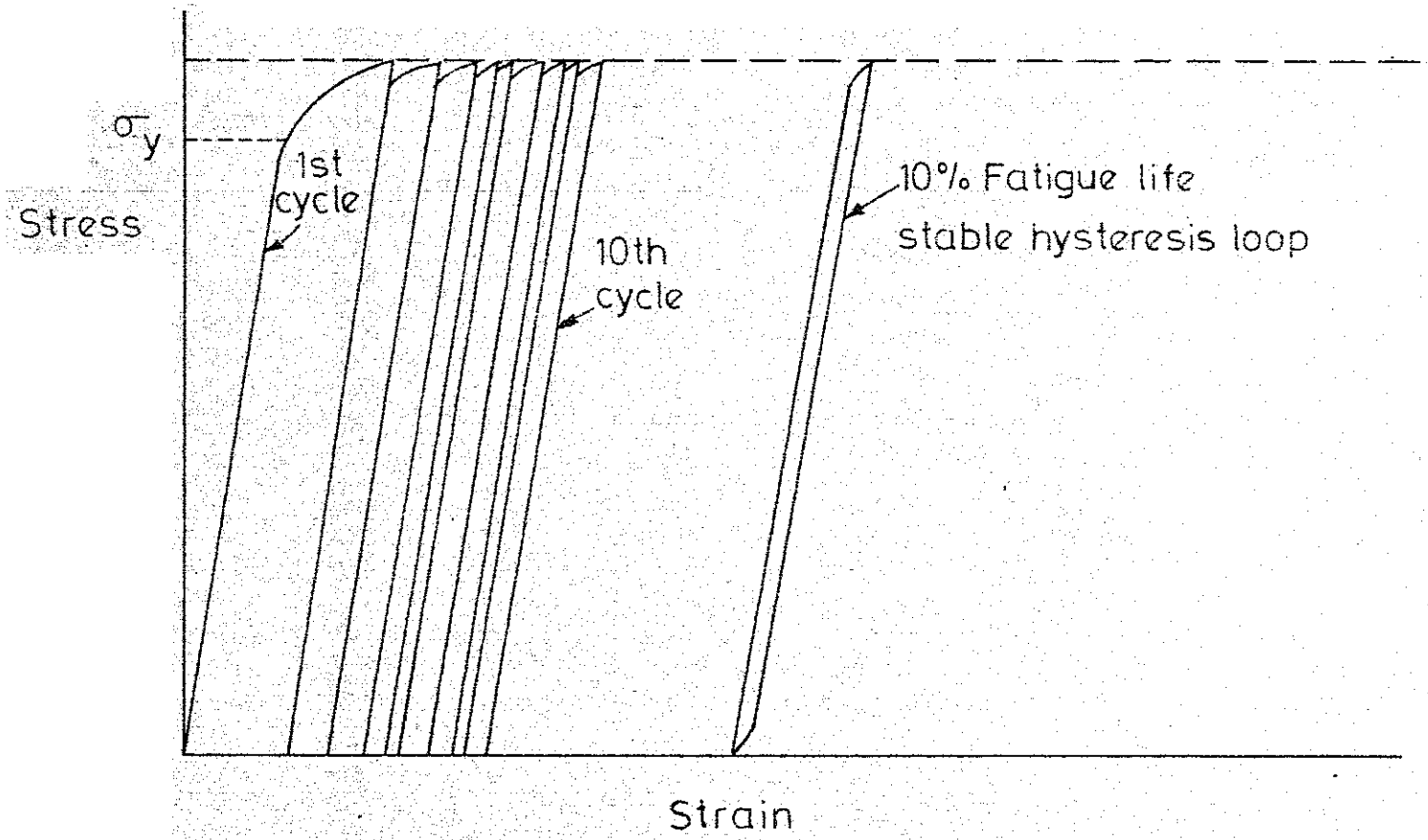

Fig.1.3 - The stress strain behaviour of a ductile metal subjected to pulsating tension fatigue.

1.5 Fracture:

Fracture in solids is initiated by some flow or imperfection which causes the high elevation of stress in that region and at this high stress, the atomic bonds at the crack edge may be broken and the flow may grow into a sizeable fracture surface causing complete failure of the solid. Cracks of brittle fracture in solids may be regarded as surfaces of discontinuity of the displacement vector $\bar{u}$. On such a surface all three components $\bar{u}_x$, $\bar{u}_y$ and $\bar{u}_z$ of this vector may suffer discontinuities. Irwin (1957) observed that there are three independent kinematic movements of the upper and lower crack surfaces with respect to each other. These deformations are illustrated in Fig. 1.4.

Case (i) Opening Mode:

It is characterized by the motions of the crack surfaces that tend to separate symmetrically with respect to the plane occupied by the crack prior to deformation.

Case (ii) Sliding Mode:

It concerns local deformation in which the crack surfaces glide over one another in opposite directions but in the same plane.

Case (iii) Tearing Mode:

It can be related to the warping action of non-circular cylinders under torsion in which the material points, initially

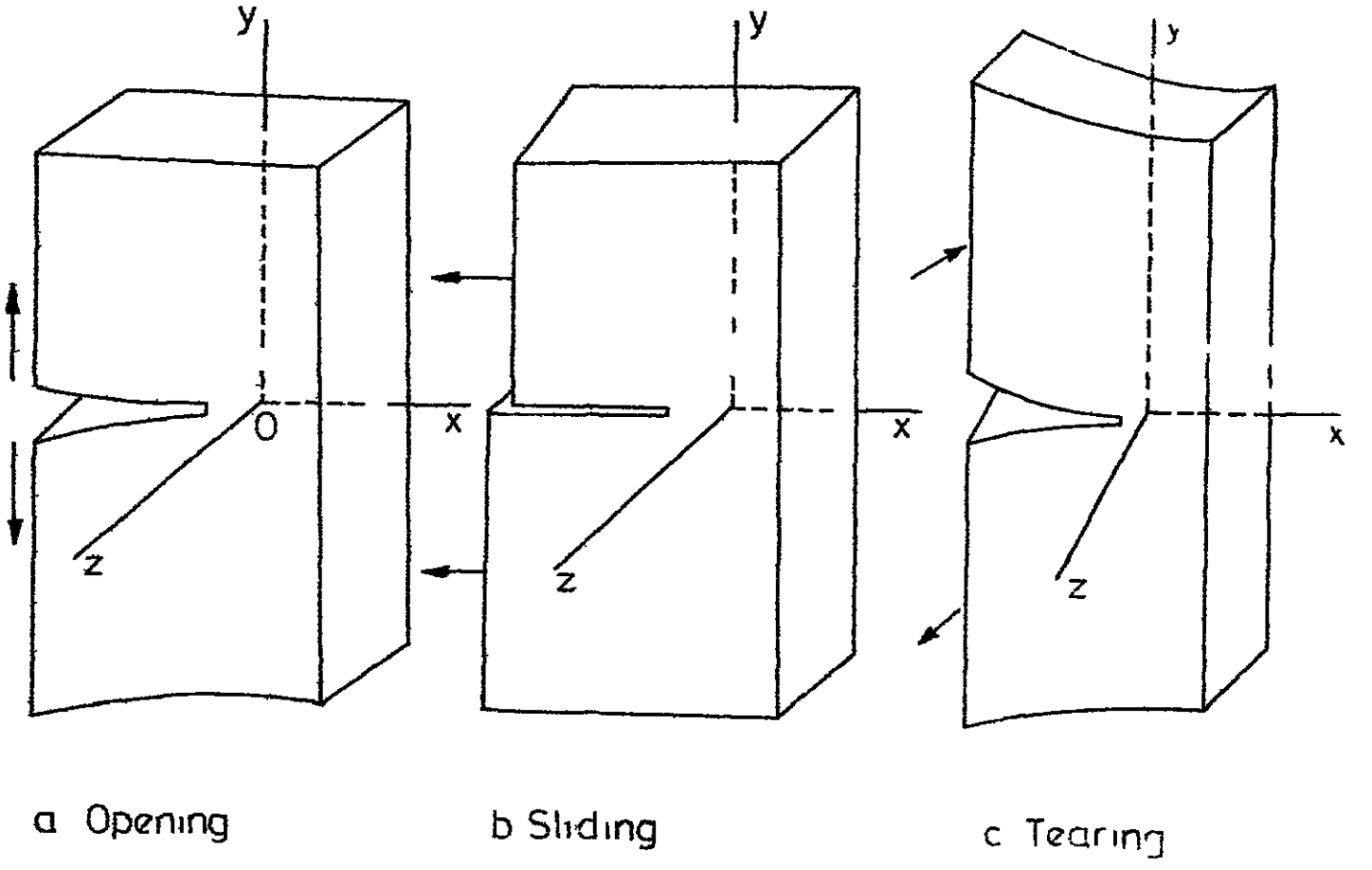

Fig 1 4 - Basic modes of crack extension

in the same plane, occupy different planes after deformation.

Each of the three crack movements is associated with a stress field in the immediate vicinity of the crack edge.

1.6 Objective of the Present Work:

The present investigation is carried out to study the nature of the fatigue crack propagation at low strain rate cycling. This investigation examines the validity of fatigue crack propagation laws in Aluminium and Mild Steel at room temperature. The empirical relations governing fatigue crack propagation rate in these two materials is reported.

The plane strain crack toughness of Aluminium and Mild Steel is also determined experimentally at room temperature conditions.

* * *

CHAPTER II

LITERATURE REVIEW

2.1 Theories of Crack Propagation:

Crack propagation theories can be classified as follows:

1. Microstructural theories
2. Macroscopic or continuum theories or Quantitative theories

Microstructural theories are based on slip movements taking place in the slip bands and resulting in the formation of intrusions and extrusions. Main objective of these theories is to explain the mechanism of formation of fatigue cracks and their propagation. This has been briefly explained in Chapter I.

Quantitative theories are based on the continuum models and are mostly semiempirical in the sense that they contain constants which have to be determined experimentally. These are two major categories of quantitative theories.

1. Dynamic crack propagation theories
2. Fatigue crack propagation theories

Dynamic crack propagation theories are based on (i) the concept of modulus of cohesion proposed by Barenblatt(1) and (ii) various forms of energy balance theory based essentially on the ideas proposed by Griffith (2).

The existing fatigue crack propagation theories deal, almost exclusively, with the propagation of fatigue cracks in thin plates under symmetric plane extensional loads and consider only the effects of mechanical continuum variables. The results are invariably expressed by a model of the form:

$$\frac{da}{dn} = f(\sigma, a, c) \qquad \ldots (2.1)$$

where $\frac{da}{dn}$ is the crack growth rate, σ represents the external loads (usually the range value of the cyclic stress), a is the half crack length and c is a material constant to be determined experimentally.

2.2 Various Continuum Models:

Deforest and Magnuson (3) studied the growth of fatigue cracks and their experiments indicated that fatigue studies were often not conclusive. It was the failure to distinguish between (i) the stresses and cycles that initiate cracks and (ii) the stresses and cycles that propagate the cracks to complete fracture.

One of the earlier continuum models is due to Head (4). He considered an infinite plate with a central crack of length 2a, subjected to one-dimensional repeated loads with the range value σ. Assuming rigid plastic work-hardening elements ahead of the crack tip, he arrived at the following relationship

$$\frac{da}{dn} = \frac{c_1 \sigma^3 a^{3/2}}{(\sigma_{ys} - \sigma) p^{1/2}} \qquad \ldots (2.2)$$

where σ_{ys} is the yield stress, p is the plastic zone size, and c_1 is a constant depending upon the mechanical properties of the material to be determined experimentally. p was assumed to be constant during the propagation of the crack.

Frost and Dugdale (5) pointed out that plastic zone size p is not independent of the crack length and is proportional to σ^2 a. They concluded, on the basis of dimensional analysis, that crack growth rate da/dn is linearly dependent on the crack length and also observed from experimental data that da/dn is proportional to σ^3, and hence proposed the following model:

$$\frac{da}{dn} = c_2 \sigma^3 a \qquad \ldots(2.3)$$

where c_2 is the characteristic parameter of the material.

Liu (6), in 1961, also using dimensional and similarity analysis arrived at the conclusion that

$$\frac{da}{dn} = F(\sigma, \sigma_m) \; a \qquad \ldots(2.4)$$

where σ_m is the mean stress.

In 1963, Liu (7) considered a hysteresis dissipation model. He further analysed the problem and pointed out that the effect of mean stress on the crack propagation is not significant. He found out that F is proportional to σ^2 and gave the following expression:

$$\frac{da}{dn} = c_3 \sigma^2 a \qquad \ldots(2.5)$$

McEvily and Illg (8) argued that due to work-hardening under cyclic load the local stress ahead of the crack tip is raised to the fracture level which leads to the rupture and hence, the crack growth rate $\frac{da}{dn}$ is a function of the maximum stress around the crack tip i.e.

$$\frac{da}{dn} = f(\sigma_{max}) \qquad \ldots(2.6)$$

By assuming the crack to be a flat elliptical hole, σ_{max} may be expressed as

$$\sigma_{max} = \left[1 + 2 (a/\rho)^{\frac{1}{2}}\right] \sigma \qquad \ldots(2.7)$$

where ρ is the radius of curvature at the tip region of the crack. McEvily and Illg (9) analysed the experimental results on the aluminium - Copper alloys and established the following empirical relation

$$\frac{da}{dn} = \log_{10}^{-1} \left(0.0051 \sigma_{max} - 5.472 - \frac{34}{\sigma_{max}-34}\right) \qquad \ldots(2.8)$$

Hardraft and McEvilly (10) pointed out that equation (2.6) may be considered to be a function of K, the stress intensity factor ($\sigma\sqrt{a}$). It is seen from equation (2.7) that

$$\sigma_{max} \simeq 2K/\sqrt{\rho} \qquad \text{as} \quad 1 \ll 2(a/\rho)^{\frac{1}{2}}$$

This point was independently observed by Paris (11,12,13) The stress intensity factor is a parameter, representing both

geometry and the external loads, and is a true measure of the stress state around the crack tip. Hence, it is the most important factor affecting the crack growth rate.

Similar continuum models have been developed by McEvily and Boettner (14), Schijve (15), Paris and Erdogan(16), Rice (17) and Valluri (18). On the basis of broad range of data it was concluded that

$$\frac{da}{dn} = c_4 K^4 \qquad \ldots(2.9)$$

where the constant c_4 is a function of material properties and external load variations.

2.3 Plastic Deformation Ahead of a Fatigue Crack:

McEvily has pointed out that the crack growth rate would be proportional to the energy stored in the plastic zone. Assuming that the density of this energy around the crack tip can be represented by K^2 and the relevant volume of the plastic zone by that of a rectangular strip ϵp ahead of the advancing crack one obtains

$$\frac{da}{dn} \simeq K^2 \epsilon p \qquad \ldots(2.10)$$

where ϵ is constant and p is the plastic zone size. For small values of p it can be shown that p is proportional to K^2 and hence equation (2.10) reduces to equation (2.9).

If p/a is not small, p is no longer proportional to K^2 and for this some new models have been developed by Rice (19), Fleck and Anderson (20) and Liu and Iino (21). The most

important is that of Rice who has given the expressions for the plastic zone and crack propagation rate, taking into account the plastic displacements of the discrete surface of tensile yielding per load cycle and the height of the rigid plastic elements in front of the crack.

2.4 Effect of Energy Dissipation on Fatigue Cracks:

If the dissipation zone ahead of the crack tip is small, the available energy to be used to overcome the dissipation around the crack tip can be obtained from:

$$\dot{U} - \dot{V} \quad \dot{T} = \dot{E}_c$$

where $\dot{U}$, $\dot{V}$ and $\dot{T}$ are respectively the time rates of external work, elastic energy and kinetic energy for a small region surrounding the crack tip and $\dot{E}_c$ is the rate of crack closure energy. If $\dot{D}$ is the rate of dissipative energy. Then at constant velocity crack growth, is $\dot{E}_c = \dot{D}$. At a certain crack velocity if $\dot{E}_c$ is greater than $\dot{D}$, the excess energy will be used to accelerate the crack.

The crack will propagate in the direction of maximum $\dot{E}_c/\dot{D}$ ratio. Probably, it may explain the existence of the curved crack and cracks with irregular shapes. If $\dot{D}$, the dissipation rate around the propagating crack, is an increasing function of velocity, $\dot{D}$ may also depend upon the crack length.

E_c is a linear function in time and also an increasing function of velocity upto a certain velocity. Near the fracture velocity, it may be possible that a further increase

in the crack velocity would cause steep increase in $\ddot{D}$ and combined with other effects at the crack tip, the total dissipation $\dot{D}$ in a forked crack may give a greater $\ddot{E}_c/\dot{D}$ ratio. In this case the crack would branch and propagation of each branch would, in turn, be governed by the respective $\ddot{E}_c/\dot{D}$ ratios in the resulting dynamic problem with the new geometry.

* * *

CHAPTER III

EXPERIMENTAL WORK

3.1 Selection of the Materials:

The experiments have been carried out on aluminium and mild steel as these are the usual structural materials and extensively used in engineering design. These materials are ductile; mild steels show a sharp knee in S-N curve while aluminium does not. The behaviour is depicted in Figure 3.1(a) and (b). Therefore in mild steel the endurance limit is sharply defined while in aluminium this limit is difficult to set as this material has distinct life at each fatigue stress level. Taking into account this basic difference, aluminium and mild steel have been chosen for studying the fatigue crack propagation rates.

3.2 Design of Specimens:

The designof test specimens for the study of crack propagation was based upon the recommendations of American Society for testing materials as described in ASTM STP 410(22) and ASTM STP 381 (23). These specifications basically are meant for the determination of valid plane strain crack toughness of any material. The dimensions of the specimen used are shown in Figure 3.2. The mild steel and aluminium specimens were identical. The specimens were loaded in tension with tension-tension fluctuating cycle as shown in Figure 3.3.

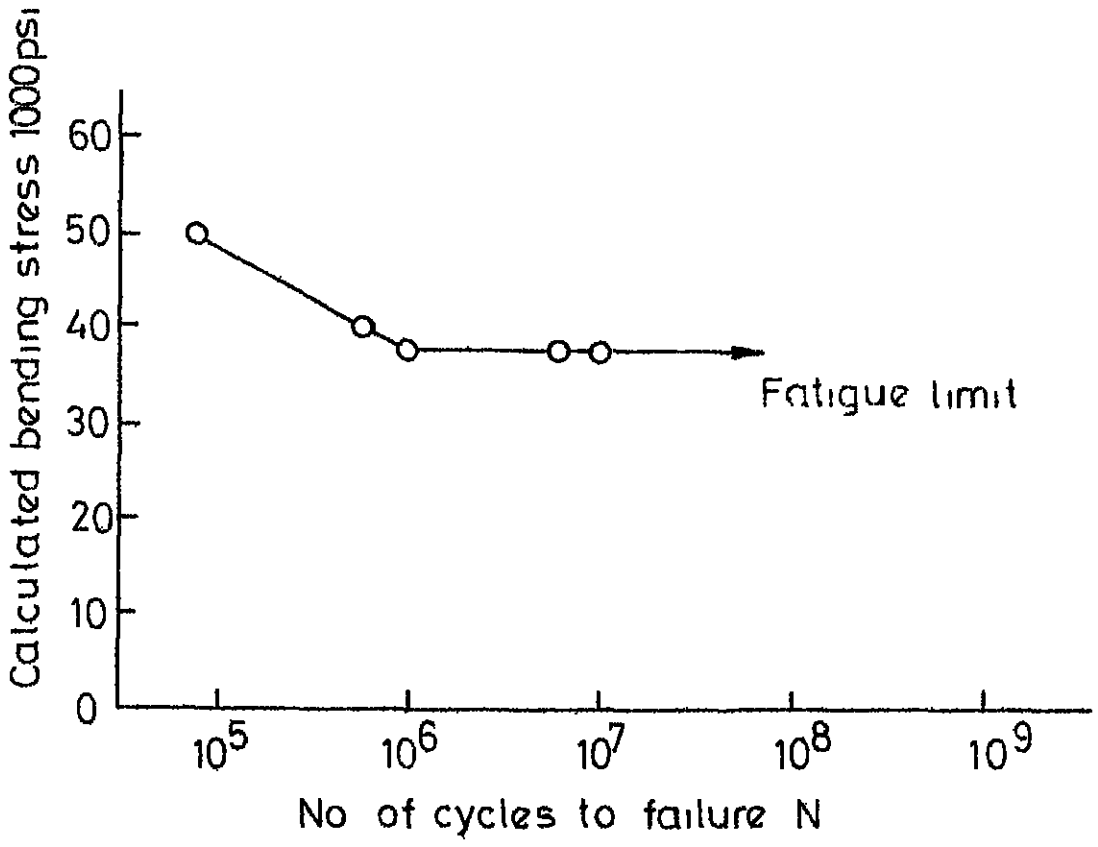

Fig 3 1a

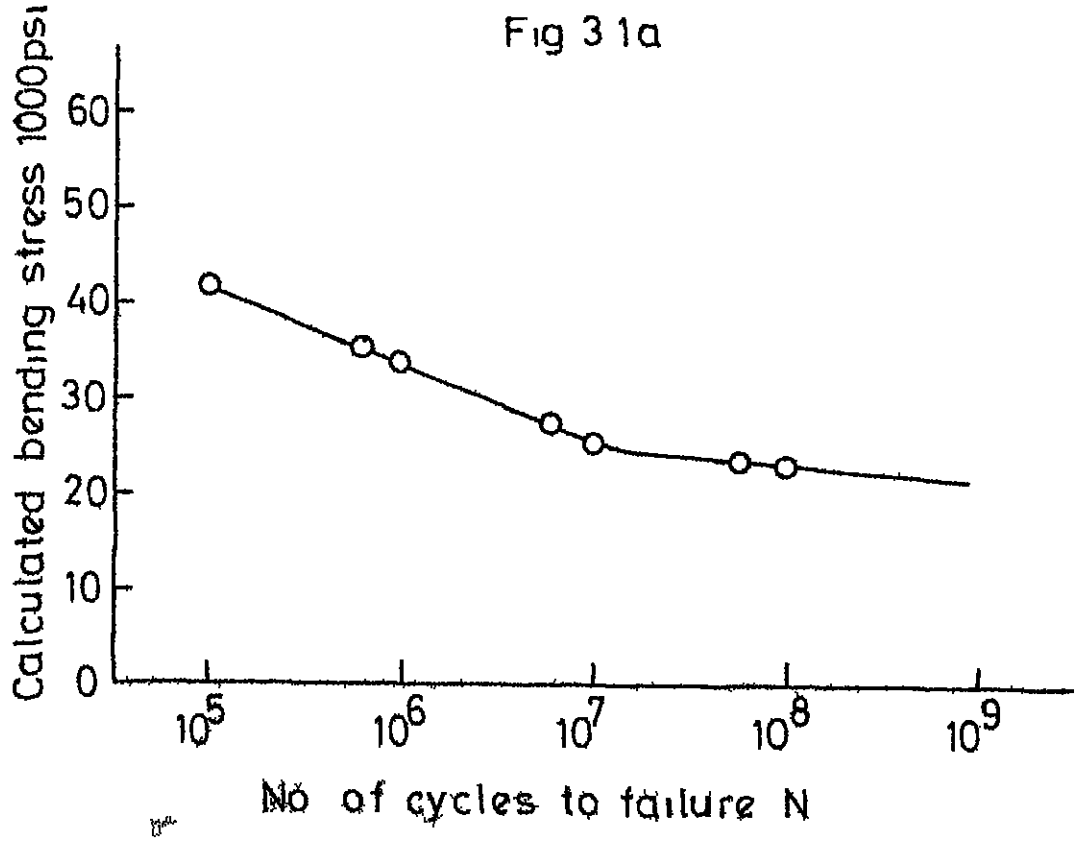

Fig 3 1b

Typical fatigue curves for ferrous and non-ferrous metals

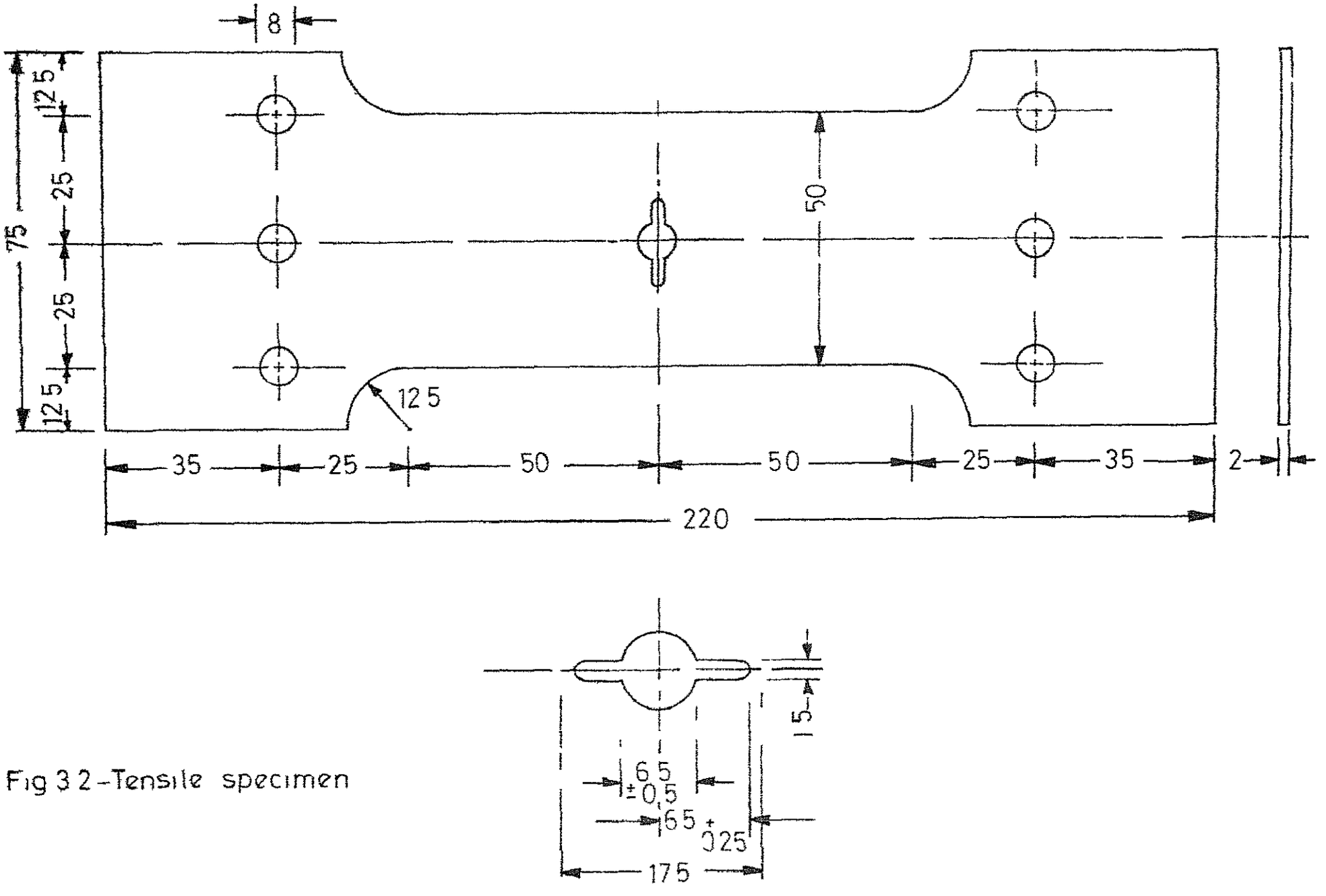

Fig 3 2 – Tensile specimen

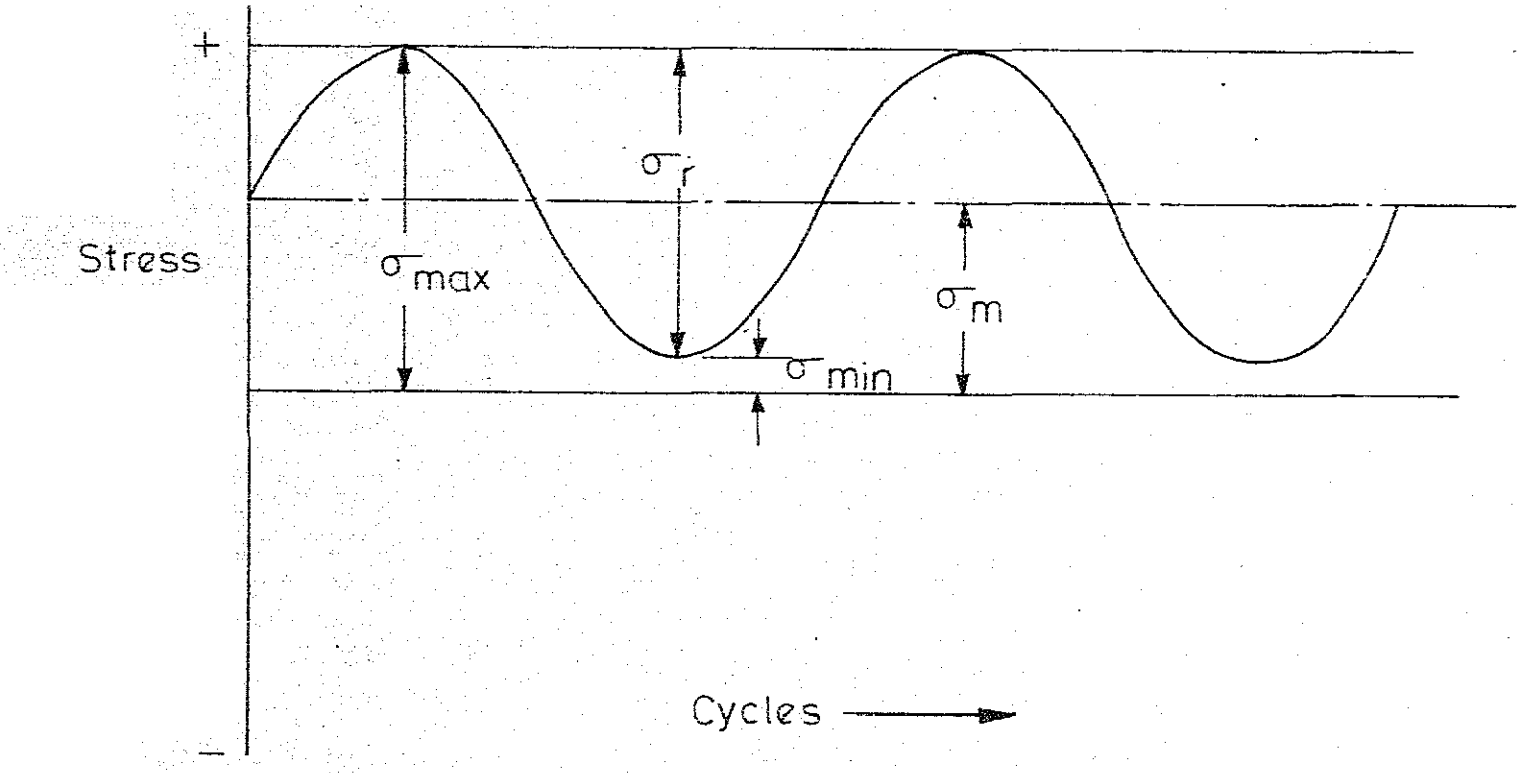

Fig. 3.3

3.3 Test Fixtures

The fixtures used for fatigue loading are shown in Figure 3.4 and plate 3.1. The fixtures made in mild steel were designed on the basis of infinite life. Three pins were used in top and bottom of the specimen respectively for getting most uniform distribution of load on the specimen. The pins were made in high carbon steel. The tests were performed in Instron Universal Instrument of 5000 kg capacity. The tests were carried out at low frequency as dictated by the machine characteristics. The frequencies were in the range of 5 cycles/min to 15 cycles/min depending upon the load.

3.4 Experimental Procedure:

One specimen was initially tested in simple tension and the breaking load for the specimen was determined for each material. Also stress-strain diagrams of both the materials were obtained as shown in Figures 3.4 and 3.5.

The specimen before putting for the experimentation was polished according to the specifications of ASTM STP 410 (22). The starting maximum load for the specimen was set around 50% of the breaking load and the minimum approximately 1/6th of the maximum load in case of aluminium and 1/3rd in case of mild steel.

The specimen was removed from the machine after each 5000 cycles and the observation was made at the tip of the notch

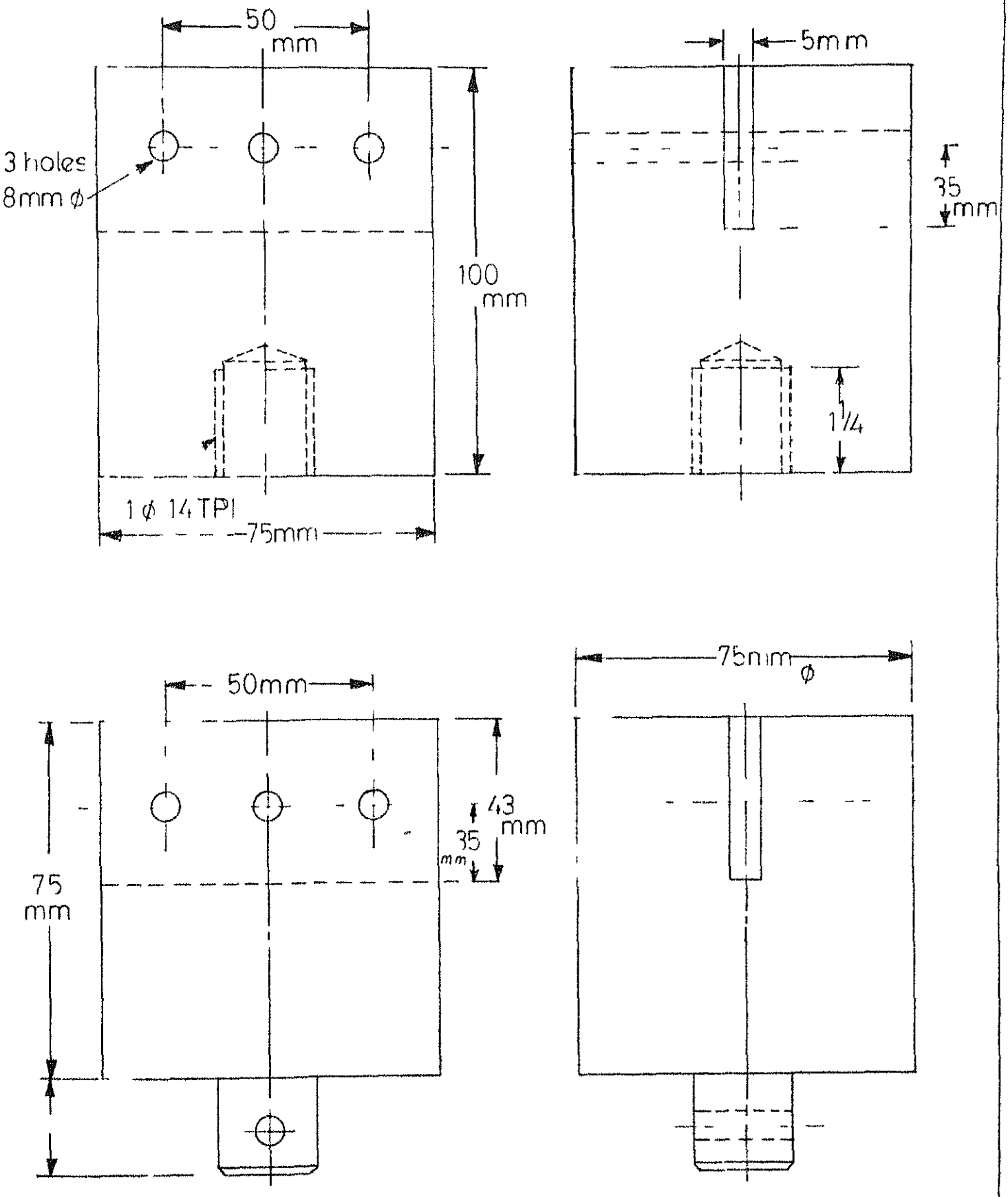

Fig 3.4(a) - Test fixtures - specimen holders

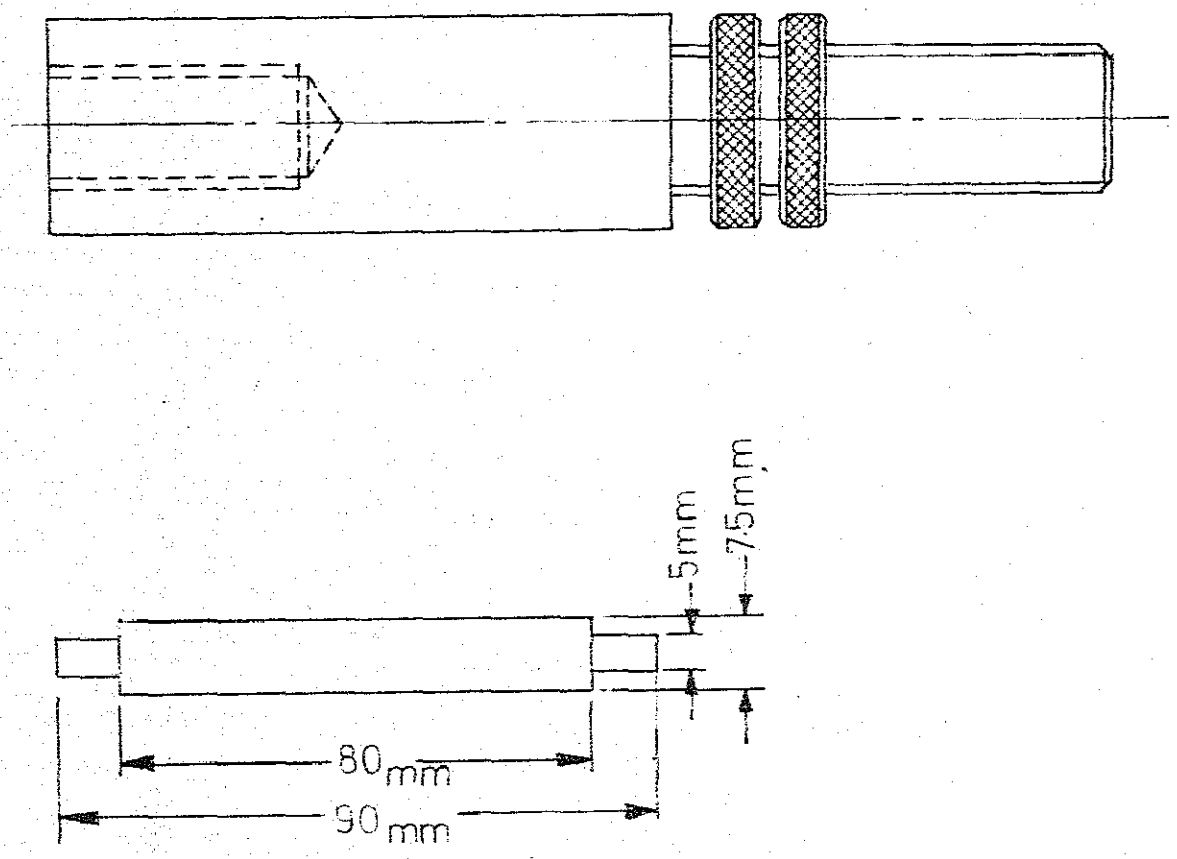

Fig.3.4(b)- Test fixtures - socket and pin.

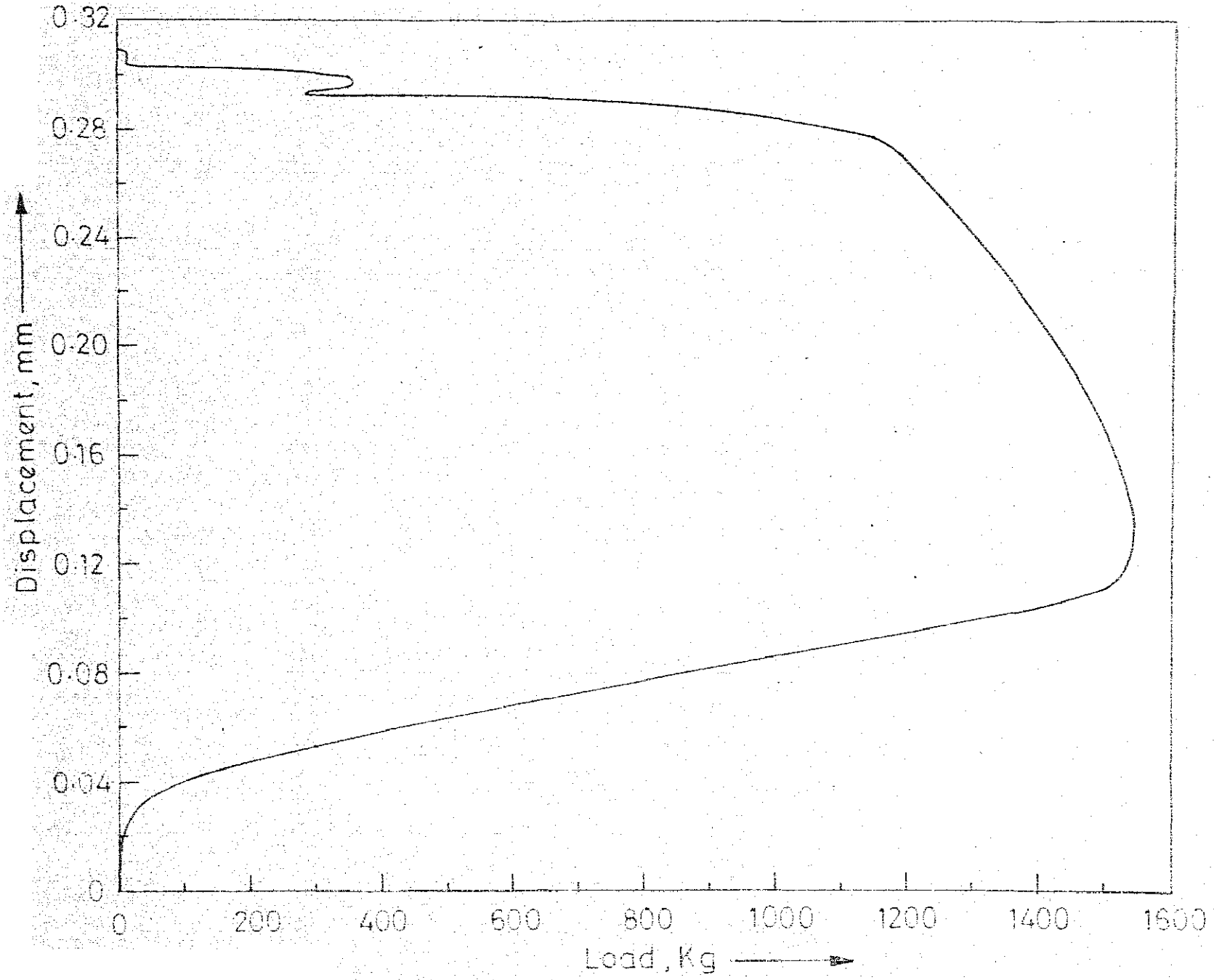

Fig. 3.5 - Load displacement diagram for Aluminium.

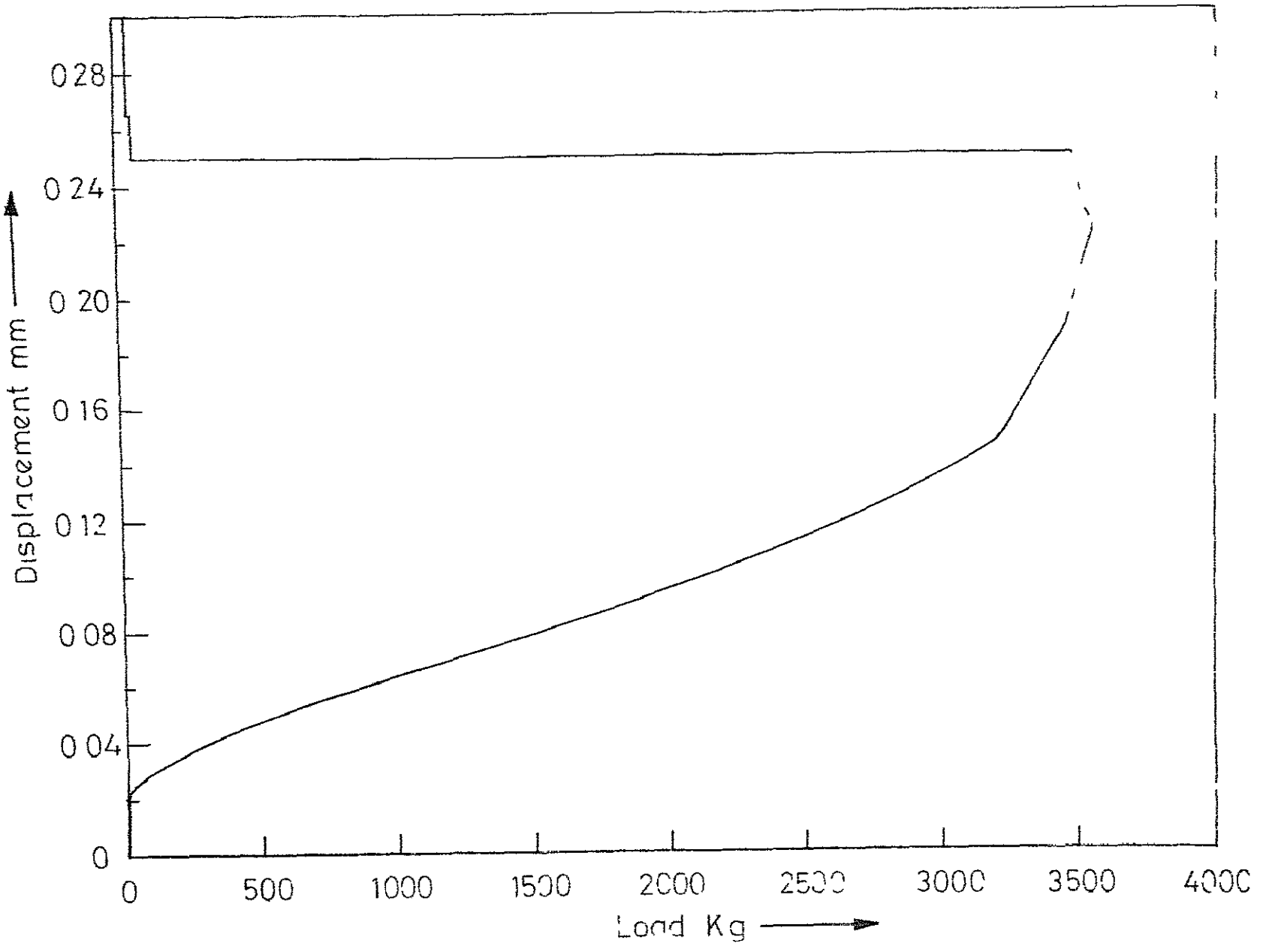

Fig 3.6 - Load displacement diagram for MS

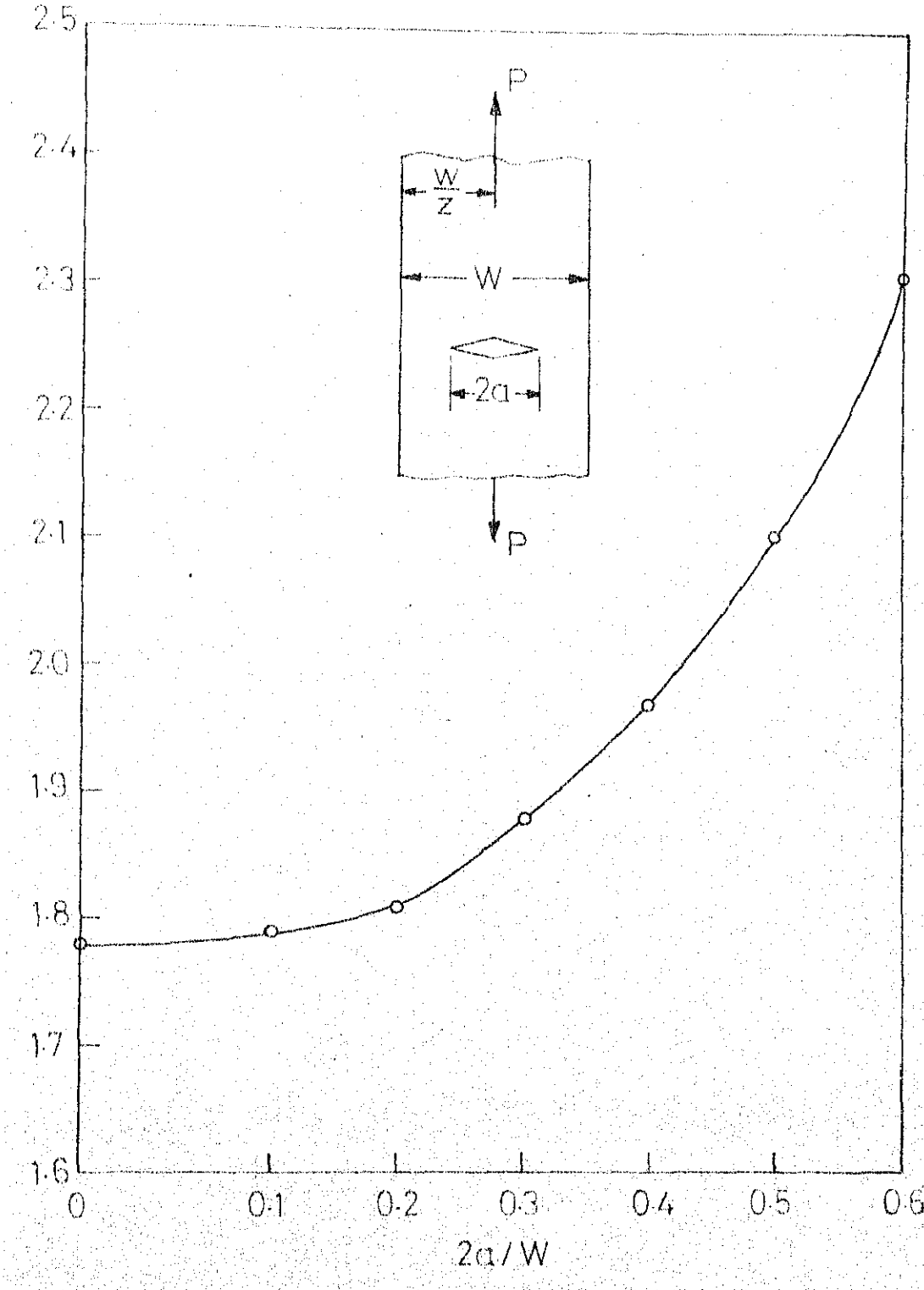

Fig 3·7 - Calibration for the centre-cracked specimen.

under the microscope with 100 or 200 magnification. The maximum load was increased in small steps till the crack became visible at the tip of the notch. As soon as the crack reached a length between 0.01 to 0.03 mms in the specimen, the maximum and minimum loads were noted and the stress intensity factor K was calculated at maximum and minimum load. ΔK, the range of stress intensity factor was also determined. The specimen was again loaded and after fixed number of cycles, the crack length was measured and the maximum load was set to keep the value of ΔK constant. The minimum load is usually determined by the specimen-fixture rigidity. The minimum load was 50 kg. After taking 5 to 6 readings for this constant ΔK, the loads were again adjusted for the other value of ΔK and another set of readings were obtained. In this way several observations were made for ΔK, crack length and number of cycles. Rate of crack propagation was then calculated for each value of ΔK and a plot was made between the rate of crack propagation and ΔK. A sample calculation for ΔK as well as crack propagation rate has been shown in Appendix II. The test-observations and results are tabulated in Appendix III.

Crack toughness, tensile test data and chemical analysis of both the materials are incorporated in Appendix I.

* * *

CHAPTER IV

DISCUSSION AND CONCLUSION

Discussion of Test Results:

(a) For different values of ΔK, the plots have been prepared for the half crack growth 'a' and number of load cycles 'n' as shown in Figure 4.1(a) and (b). It is clear from these figures that at low values of ΔK, the increase in 'a' is very small and as ΔK increases the rate of increase of 'a' also increases.

In case of aluminium, the ΔK was varied between the maximum value of 23.65 $Kg/mm^2 \sqrt{mm}$ to 8.85 $Kg/mm^2 \sqrt{mm}$ in 22 steps. The value of ΔK remained constant during each step and variation of 'a' with 'n' at constant ΔK is shown in Figure 4.1(a). From this figure it is clear that the curves become steep beyond $K = 19\ Kg/mm^2 \sqrt{mm}$ while the slope of the curve at point 'A' when $K = 8.5\ Kg/mm^2 \sqrt{mm}$ is in the range of 0.8×10^{-6} mm/cycle. Below this value of ΔK no crack propagation was observed even for 10,000 cycles.

In case of mild steel also the curves become steeper as value of ΔK increases, but no sudden change in slope was observed at any value of ΔK in the region of ΔK for which the experiment was performed.

(b) The law for the rate of fatigue-crack propagation in both the metals, aluminium and mild steel, has been investigated in a particular range of ΔK at low strain rate cycle. The

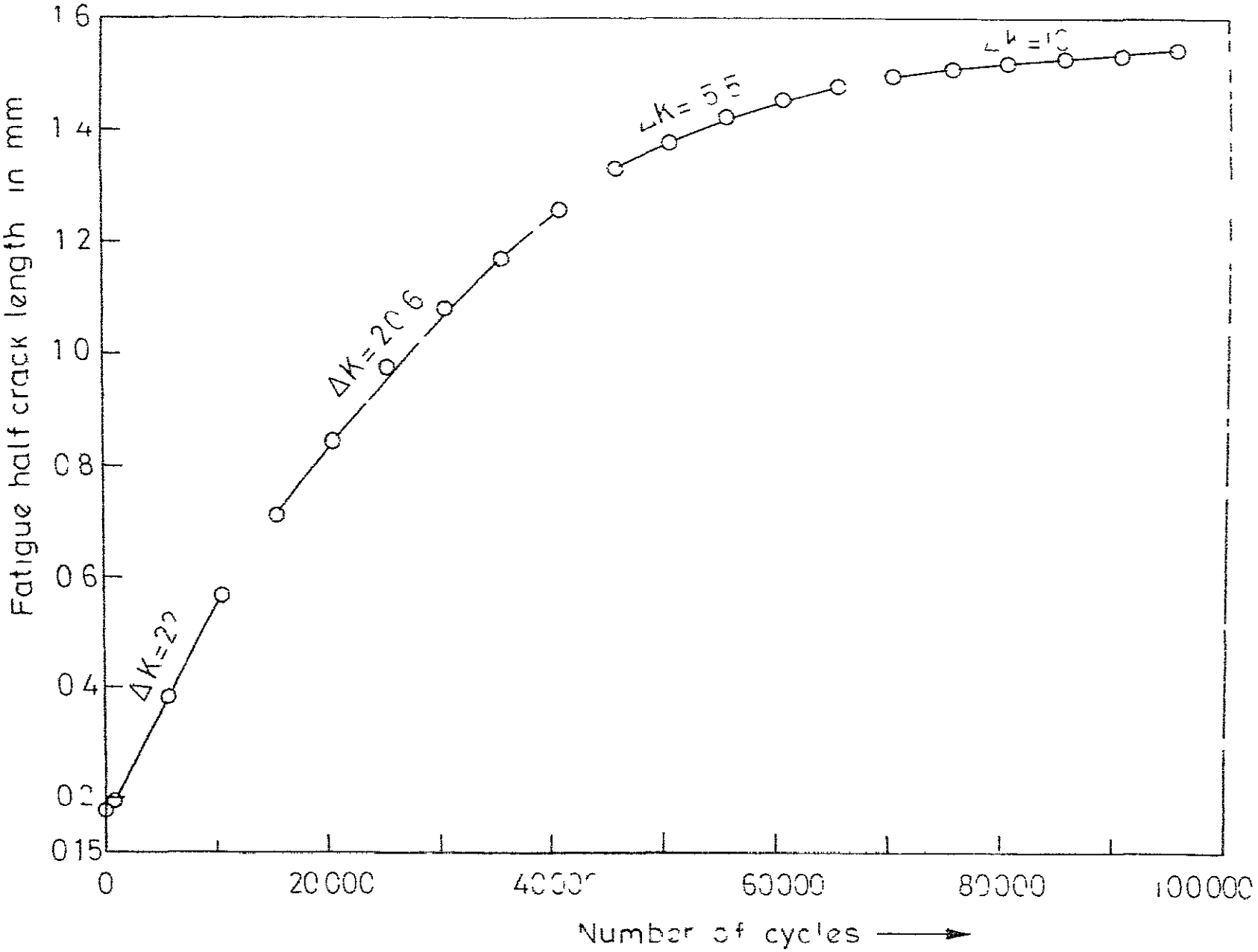

Fig 4 : (a) - Variation of crack length with number of cycles at various values of stress intensity factors in Aluminium

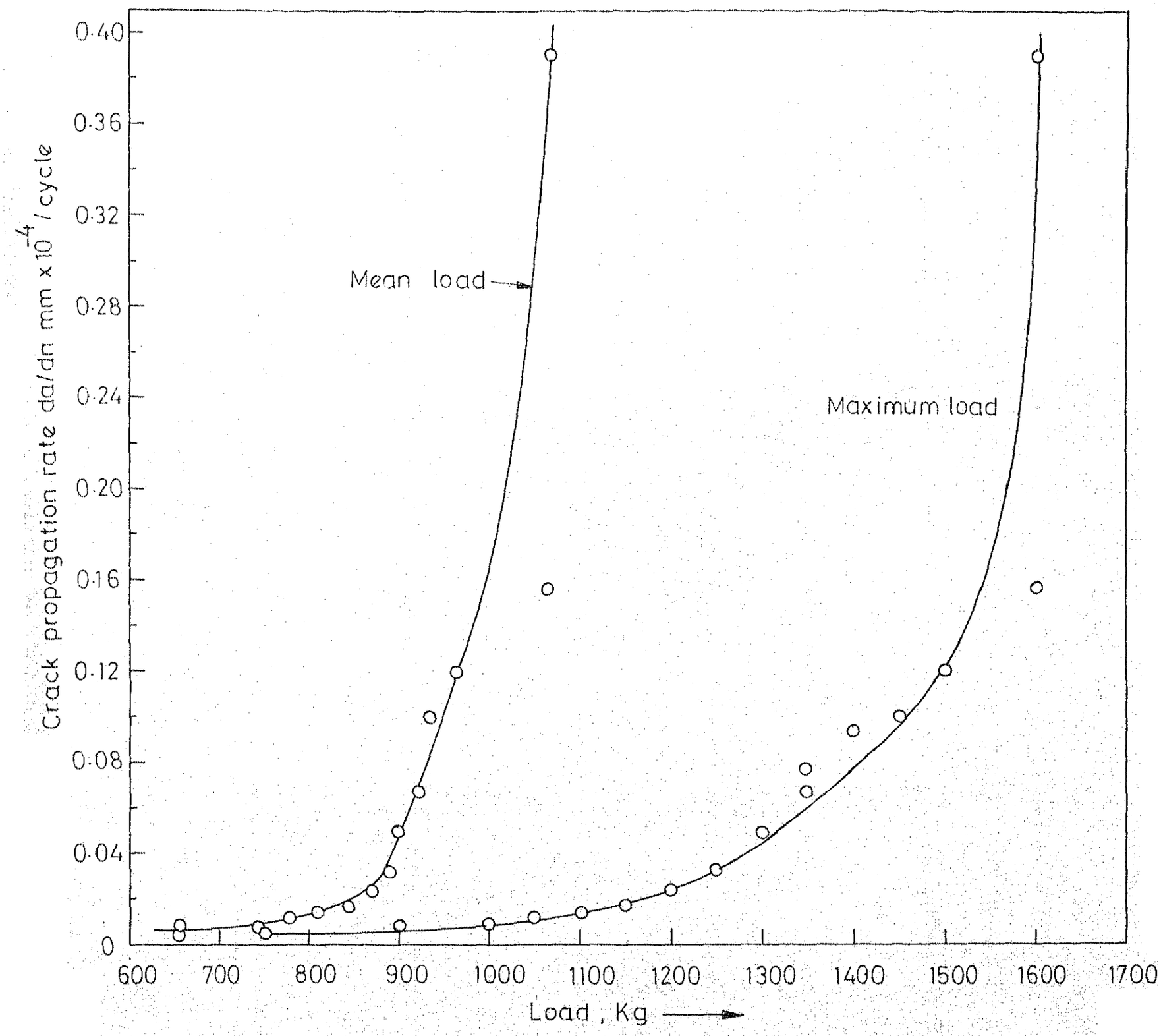

Fig. 4·3(b) - Variation propagation rate with maximum and mean loads

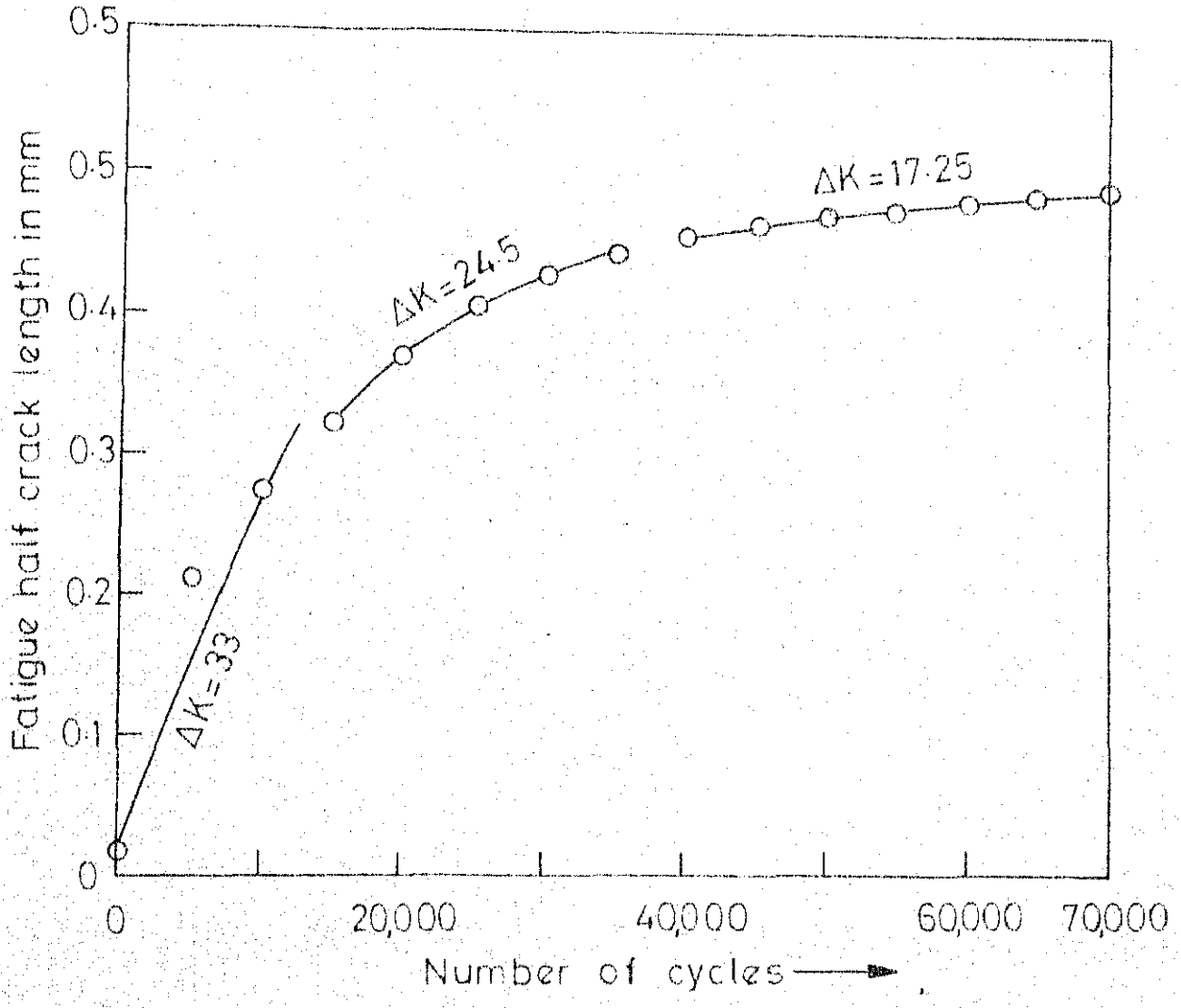

Fig.4.1(b)-Variation of crack length with number of cycles at various values of stress intensity factors in M.S.

The range of ΔK has been selected from the consideration of practical application of these data and the limitations of Instron Instrument.

The plots of crack growth rate (da/dn) vs range of stress intensity factor (ΔK) were made on log-log paper for both the metals. These are shown in Figure 4.2(a) and 4.2(b). It was found that for both the metals, the straight lines can be fitted in log-log plots of (da/dn) vs (ΔK). Furthermore, in aluminium, the range of (ΔK) could be divided into two parts. In the region of low values of (ΔK), the slope of straight line is less while in the region of higher values of (ΔK) the straight line becomes steeper. The value of (ΔK) at which both these lines intersect is of considerable importance as this is the point when the constants of the crack-growth laws change.

In case of aluminium this value of (ΔK) is 19 $Kg/mm^2 \sqrt{mm}$ as is seen in Figure 4.2(a). In the lower region, K varies from 8.83 $Kg/mm^2 \sqrt{mm}$ to 19 $Kg/mm^2 \sqrt{mm}$ and in the higher region from 19 $Kg/mm^2 \sqrt{mm}$ to 23.16 $Kg/mm^2 \sqrt{mm}$. The fatigue crack growth rate law can be expressed as follows:

$$\frac{da}{dn} = C (\Delta K)^m \qquad (4.1)$$

The values of constants C and m are given in Table 4.1.

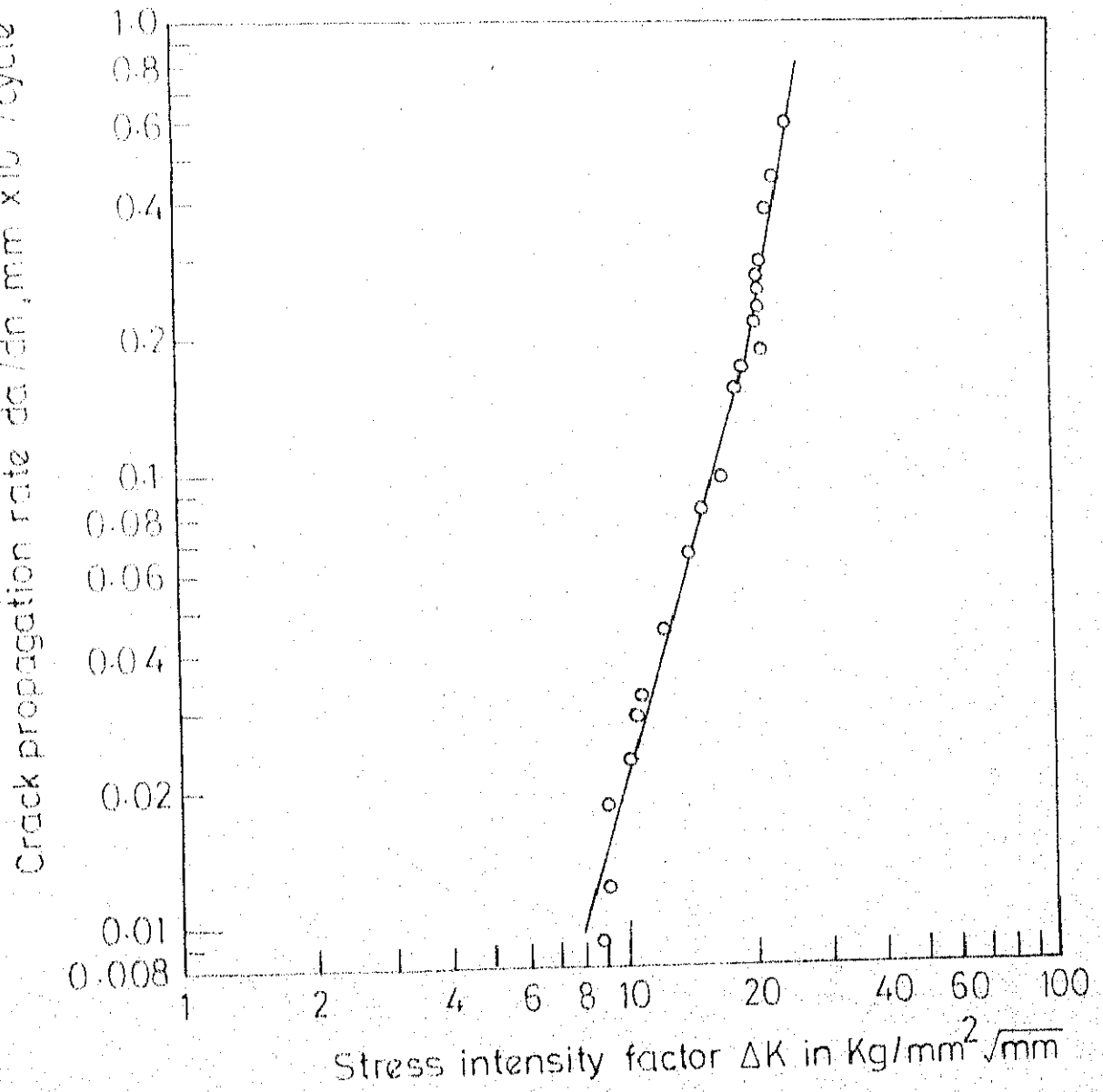

Fig.4.2(a) - Variation of crack propagation rate with stress intensity factor for ~~M.S.~~ Aluminium

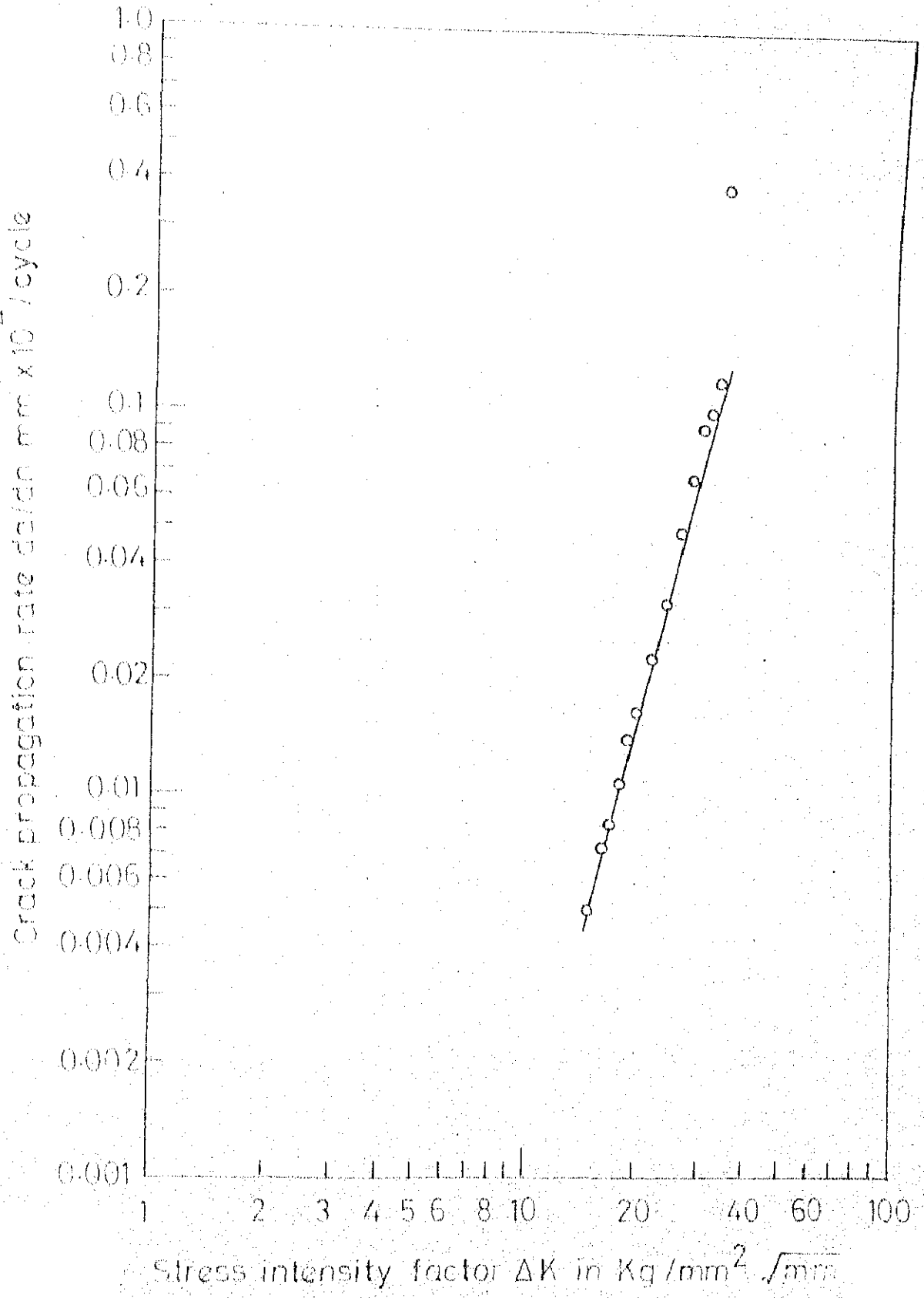

Fig.4.2 (b) - Variation of crack propagation rate with stress intensity factor for ~~Aluminium~~ Mild Steel

TABLE 4.1

CONSTANTS C and m for Aluminium

Range of ΔK ($Kg/mm^2 \sqrt{mm}$)	m	C
8.83 to 19.00	3.13	8×10^{-12}
19.00 to 23.16	4.66	

It can be seen from Figure 4.2(b) that $(\frac{da}{dn})$ vs (ΔK) plot for mild steel can not be divided into two distinct straight lines as in the case of aluminium. Although some earlier investigators (21) have tried to fit two straight lines in the case of mild steel in annealed condition; yet these two straight lines did not differ very much in slopes. From present results it can be concluded that within the range of (ΔK) for which the tests were performed,(da/dn) vs (ΔK) constitutes only one straight line,the constants of which are presented in Table 4.2.

TABLE 4.2

CONSTANTS C and m for Mild Steel

Range of ΔK ($kg/mm^2 \sqrt{mm}$)	C	m
15.00 to 35.00	9.52×10^{-8}	3.96

Conclusions:

Following conclusions have been drawn from the present study:

(i) Crack-growth rate increases sharply for values beyond $\Delta K = 19.00$ Kg/mm^2 $\sqrt{mm}$ in the case of aluminium.

(ii) For mild steel, in the region of ΔK studied, a single power law can be fitted with sufficient accuracy. It was found that the value of index of power law is 3.96 for $\Delta K = 15$ to 35 Kg/mm^2 $\sqrt{mm}$.

(iii) In case of aluminium, in the region of ΔK studied, similar power laws can be fitted with sufficient accuracy. The value of index of power law was found to be 3.13, in the region of ΔK 8.83 to 19 Kg/mm^2 $\sqrt{mm}$ and 4.66 in the region of ΔK 19 to 23.16 Kg/mm^2 $\sqrt{mm}$.

(iv) The plane strain crack toughness of both aluminium and mild steel are also reported at room temperature.

Suggestions for Further Work:

Further work should be carried out to study the effect of

i) the notch geometry on fatigue-crack propagation rate

ii) sub zero and elevated temperatures on crack-propagation rate

iii) prior stressing or residual stresses on crack-propagation rate

iv) plastic zone size and plastic energy dissipation on crack-propagation rate.

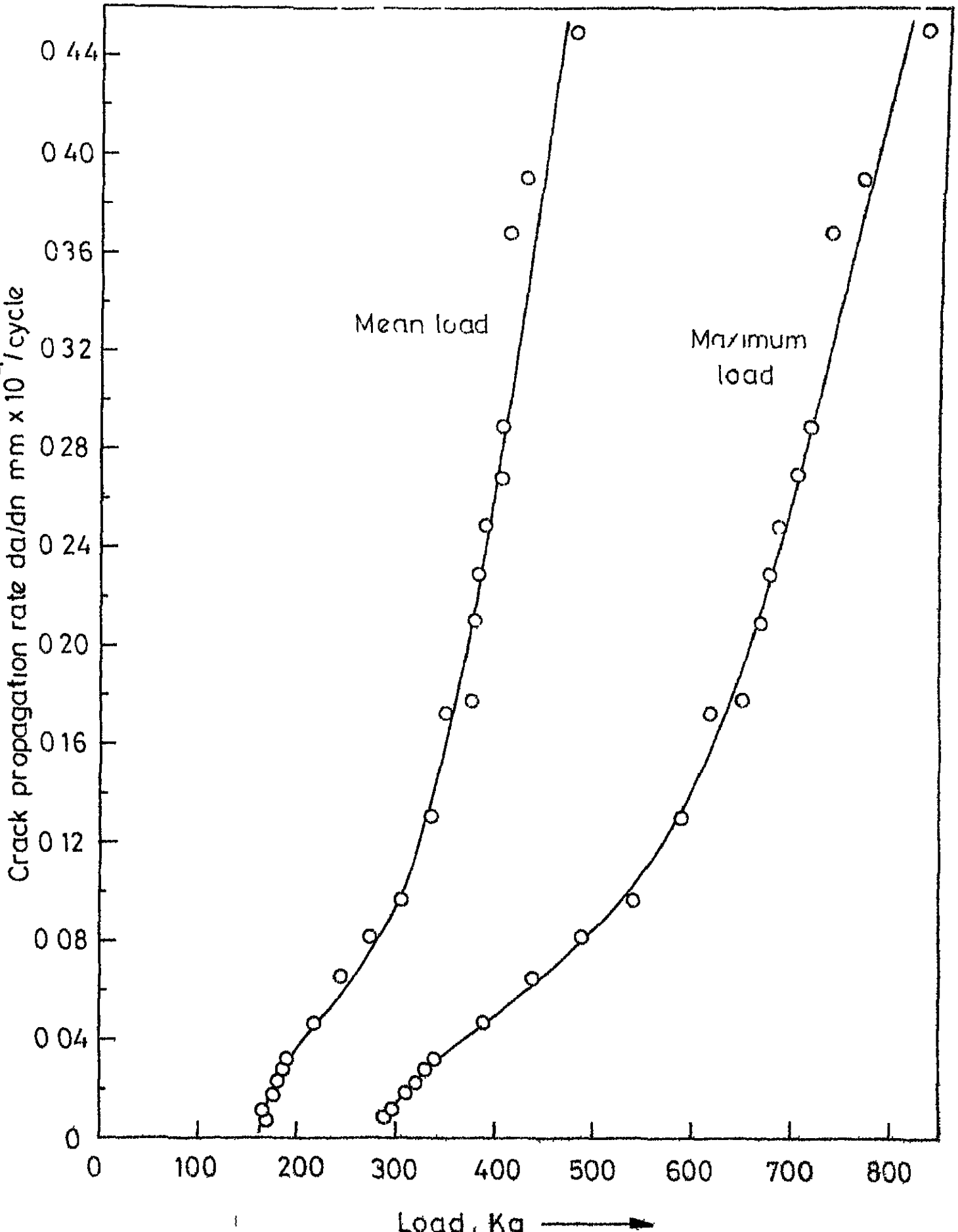

Fig 4 3(a) - Variation of crack propagation rate with maximum and mean loads in Aluminium

REFERENCES

1. Barenblatt's work cited in Fracture, Vol. II, by Liebowitz, H., p. 22, 1968.
2. Griffith's work cited in Fracture, Vol. II, by Liebowitz, H., p. 18, 1968.
3. Deforest, A.V. and Magnusan, F.W., "The Rate of Growth of Fatigue Cracks, Journal of Applied Mechanics, March, 1936, p. A-23.
4. Head, A.K., "The Growth of the Fatigue Cracks", The Philosophical Magazine, Vol. 44, Series 7, 1953, p.925.
5. Frost, N.E. and Dugdale, D.S., "The Propagation of Fatigue Cracks, in Sheet Specimen", Journal of the Mechanics and Physics of Solids, Vol. 6, 1958, pp.93-110.
6. Liu, H.W. "Crack Propagation in Thin Metal Sheets under Repeated Loading, Transactions, ASME, Series D (Journal of Basic Engg.), Vol. 83, No.1, 1961.
7. Liu, H.W., Fatigue Crack Propagation and Applied Stress Range, an Energy Approach, Journal of Basic Engineering, Transactions of ASME, Series D, Vol. 85, 1963, pp 116.

8,9. McEvily, A.J. and Illg, W., The Rate of Fatigue-Crack Propagation in Two Aluminium Alloys, ANCA TN 4394, September, 1958.

10. Hardrath, H.F. and McEvily, A.J., Engineering Aspects of Fatigue Crack Propagation, Proceedings of the Crack Propagation Symposium, Vol. II, Cranfield, England, October, 1961.
11. Paris, P.C., "The Fracture Mechanics Approach to Fatigue"

Fatigue-An Interdisciplinary Approach Syracuse University, Press, Syracuse, N.Y., 1964.

12. Paris, P.C., The Growth of Cracks due to Variation in Loads, Ph.D. Physics, Lehigh University, Bethlehem, Pa., 1962.

13. Paris, P.C. "A Handbook of Crack Tip Stress Intensity Factor, Lehigh University, Institute of Research, Bethlehem, Pa., June 1960.

14. McEvily, A.J. and Boettner, R.C. On Fatigue Crack Propagatio in F.C.C. metals, Acta Mettalurgical Vol. 11, 1963, p. 11.

15. Schijve, J., Significance of Fatigue Cracks in Micro-Range and Macro-Range, Fatigue Crack Propagation, ASTM STP 415, ASTM, 1967, p.415.

16. Paris, P.C. and Erdogan, A Critical Analysis of Crack Propagation Laws Trans, ASME, Series D, Vol. 85, Dec.,1963.

17. Rice, J.R., Mechanics of Crack Tip Deformation and Extension by Fatigue, Fatigue Crack Propagation, ASTM STP 415, ASTM, 1967, p. 247.

18. Valluri, S.R. "A Unified Engineering Theory High Stress Level Fatigue ARL Tech., GALCITSM 61-1, October, 1961.

19. Rice, J.R., Plastic Yielding at a Crack Tip, Proceedings, International Conference Fracture, Sendai, Japan, 1965.

20. Flack, W.G. and Anderson, R.B., A Mechanical Model of Fatigue Crack Propagation; Fracture 1969, Proceedings of Second International Conference on Fracture Brighton, April 1969, p. 790.

21. Liu, H.W. and Lino, N., Mechanical Model for Fatigue Crack Propagation Fracture 1969, Proceedings of the Second International Conference on Fracture, Brighton, April 1969, p. 812.

22. Brown, W.F., Jr., and Shawley, John E., Plane Strain Crack Toughness Testing of High Strength Metallic Materials.

23. Fracture Toughness Testing and Its Application, ASTM-STP 381, p. 190.

* **

APPENDIX II

SAMPLE CALCULATION

Consider the observation 15th in Table I Appendix III.

Observed Values:

Maximum Load P_{max} = 390 Kg

Minimum Load P_{min} = 50 Kg

Width w = 50 mm

Thickness t = 3 mm

Half fatigue crack length at 60,250, cycles a_1 = 1.453 mm

Half fatigue crack length at 65,250 cycles, a_2 = 1.476 mm

Half Notch depth a_o = 6.75 mm

Calculations:

Gross area of x-section = 50 x 3 = 150 mm^2

Increase in crack length a = (1.476 -1.453) mm

= 0.023 mm

Number of cycles for this increase in crack length = 65250 -60,250

= 5000 cycles

Fatigue crack propagation Rate = $\frac{0.023}{5000}$ mm/cycle

= 0.046×10^{-4} mm/cycle

Fatigue half crack length + Half notch depth a = $a_2 + a_o$

or a = 1.476 + 6.75 = 8.226 mm

2a = 16.452 mm.

Calibration factor $y = 1.77\left[1-0.1\left(\frac{2a}{w}\right) + \left(\frac{2a}{w}\right)^2\right]$

$= 1.77\left[1-0.1\left(\frac{16.452}{50}\right) + \left(\frac{16.452}{50}\right)^2\right]$

$= 1.908$

Maximum stress intensity factor $K_{max} = \frac{P_{max}}{\text{Gross area}} \sqrt{a}\ y$

$= \frac{390}{150} \sqrt{8.226} \times 1.908 = 14.22 \frac{Kg}{mm^2} \sqrt{mm}$

Minimum stress intensity factor $K_{min} = \frac{P_{min}}{\text{Gross area}} \sqrt{a}\ y$

$= \frac{50}{150} \sqrt{8.226} \times 1.908$

$= 1.82 \frac{Kg}{mm^2} \sqrt{mm}$

Range of stress intensity factor,

$\Delta K = (14.22 - 1.82)\ Kg/mm^2 \sqrt{mm}$

$= 12.40\ Kg/mm^2 \sqrt{mm}$

Crack Toughness for Aluminium $K_{IC} = \frac{P_{yield}}{\text{Gross area}} \sqrt{a} \times y$

$= \frac{1400}{150} \sqrt{8.287} \times 1.915$

$= 51.40\ Kg/mm^2 \sqrt{mm}$

Crack toughness for Mild Steel $K_{IC} = \frac{P_{yield}}{\text{Gross area}} \sqrt{a}\ y$

$= \frac{3250}{150} \sqrt{7.2356} \times 1.868$

$= 108.50\ Kg/mm^2 \sqrt{mm}$

ERROR ANALYSIS

There are two types of errors:

(1) Systematic Errors: These are the errors inherited in the instrument.

(2) Random Errors: These errors depend upon the least count ofthe instrument and the human judgement in taking the readings.

Errors in Linear Measurements

(i) Measurement of Fatigue Half Crack Length, a_2

This measurement was done with the help of Tucon-Hardness Tester which can read a minimum of 0.0005mm with magnification of 100 and a minimum of 0.00025mm with magnification of 200. Assuming that there is no systematic error in the machine, the percentage of random error is $\pm$ 0.235.....(.0005/0.2125)x100

(ii) Measurement of Notch Depth, a_0

A microscope with a least count 0.01mm was used to measure the length. The systematic error involved in the calibration of microscope may be assumed to be zero whereas, the random error involved may be $\pm$ 0.074...(.01/13.5x100)

(iii) Measurement of Width,w

It was measured using a vernier calliper having least count of 0.01mm. So the random error involved may be $\pm$ 0.02% .....($\pm$ 0.01/50x100)

(iv) Measurement of Thickness, t, of the specimen

Same vernier calliper was used for measuring thickness and the random error may be $\pm$ 0.33%.....($\pm$ 0.01/3 x100)

Error In Measurement Of Loads

Loads were directly recorded on the recorder attatched to the Universal Instron Instrument used in the experiment. During the experiment loads were adjusted to match a line on the load scale. Thus there was no random error involved. Systematic error was adjusted to be zero by calibrating the load scale.

Error In Counting The Number Of Load Cycles

An automatic counter was used for the purpose. It is assumed that there is no systematic error in the instrument. No random error is present because of the automatic counting system of the loading cycles.

ERROR ESTIMATES

(a) Error in Half Crack Length, a

Half crack length a = Fatigue half crack length a_2 + Half notch depth a_0

Error in a = Error in a_2 + Error in a_0

$= (\pm 0.235 \pm 0.074) \times 100$

$= \pm 0.309\ \%$

(b) Error in Z

$Z = a/w$

Error in Z = Error in a + Error in w

$= \pm 0.309 \pm 0.02$

$= \pm 0.329\ \%$

(c) Error in Calibration factor, y

$y = 1.77\left[1-0.1(2Z)+(2Z)^2\right]$

Error in $y = \delta y/y = \left[(-0.1+4Z)/(1-0.2Z+4Z^2)\right] \times 2\ dZ$

$= (-0.1 + 4.02\ Z) \times 2\ dZ$ neglecting higher powers of Z

$= (-0.1 + 4.02 \times 0.166) \times 2 \times 0.329$

$= \pm 0.373\ \%$

(d) Error in Stress Intensity Factor K_{max}/ K_{min}

$K = P\sqrt{a}\ y/\ w.t.$

Error in K = (Error in P $\pm$ Error in w $\pm$ Error in t $\pm$ 1/2 Error in a $\pm$ Error in y) x 100

$= (\pm 0.00 \pm 0.02 \pm 0.33 \pm 0.1545 \pm 0.373)\%$

$= \pm 0.8775\ \%$

(e) Error in ΔK

$\Delta K = K_{max} - K_{min}$

Error in ΔK = Error in K_{max} + Error in K_{min}

= 2 x Error in K

Error in ΔK = 2 x 0.8775 %

= $\pm$ 1.755 %

(d) Error in $\Delta a/\Delta n$

Error in $\Delta a/\Delta n$ = Error in Δa + Error in Δn

= 2 x Error in a + Error in Δn

= $\pm$ 0.618 $\pm$ 0.00

= $\pm$ 0.618 %

(g) Error in C

Error in C is the same as error in $\Delta a/\Delta n$ and is $\pm$ 0.618 %

(h) Error in m

m is the slope of the curve $\Delta a/\Delta n$ vs ΔK

Error in m = $\pm$ Error in $\Delta a/\Delta n$ $\pm$ Error in ΔK

= $\pm$ 0.618 $\pm$ 1.755

= $\pm$ 2.373 %

APPENDIX III

TEST OBSERVATIONS AND RESULTS

Sl. No.	No. of Cycles	Maximum Load, Kg $P_{max.}$	Minimum Load, Kg. $P_{min.}$	Fatigue Half crack length, mm.	Half Crack length in mm, a	Calibration Factor, y			Propagation Rate in mm. per cycle x 10^4 da/dn
1.	0000	830	130	0.182	6.932	1.858	27.45/4.29	23.16	0.451
2.	0250	770	90	0.1933	6.9433	1.858	25.01/2.84	22.17	0.381
3.	5250	740	90	0.3833	7.1333	1.865	24.58/2.99	21.59	0.370
4.	10250	720	100	0.568	7.318	1.870	24.48/3.40	21.08	0.290
5.	15250	710	100	0.713	7.463	1.872	24.20/3.41	20.79	0.270
6.	20250	690	90	0.848	7.598	1.880	23.81/3.11	20.70	0.250
7.	25250	680	85	0.973	7.723	1.885	23.73/2.97	20.96	0.230
8.	30250	670	90	1.079	7.829	1.888	23.60/3.17	20.43	0.211
9.	35250	650	100	1.168	7.918	1.890	25.05/3.55	21.50	0.179
10.	40250	620	80	1.255	8.005	1.896	22.15/2.86	19.29	0.174
11.	45250	590	80	1.331	8.081	1.900	21.22/2.88	18.34	0.151
12.	50250	540	70	1.379	8.129	1.904	19.54/2.53	17.01	0.097
13.	55250	490	60	1.420	8.170	1.906	17.80/2.18	15.62	0.082

....2

Test Observations and Results (Contd.)

14.	60250	440	50	1.453	8.203	1.908	16.04/1.82	14.22	0.066
15.	65250	390	50	1.476	8.226	1.908	14.22/1.82	12.40	0.047
16.	70250	340	40	1.492	8.242	1.910	12.44/1.46	10.98	0.032
17.	75250	330	40	1.506	8.256	1.910	12.07/1.46	10.61	0.028
18.	80250	320	40	1.518	8.268	1.910	11.71/1.46	10.25	0.023
19.	85250	310	40	1.527	8.277	1.912	11.36/1.46	9.19	0.018
20.	90250	295	40	1.533	8.283	1.912	10.65/1.46	9.19	0.012
21.	95250	290	50	1.537	8.287	1.915	10.66/1.83	8.83	0.009

TABLE 2

1.	0000	1600	530	0.0175	6.7675	-	-	-	-
2.	5000	1600	530	0.2125	6.9625	1.858	52.34/17.34	0.39	35.00
3.	10000	1500	480	0.2725	7.0225	1.860	49.30/15.78	0.12	33.52
4.	15000	1450	480	0.3219	7.0719	1.861	47.87/15.85	0.0998	32.02
5.	20000	1400	470	0.3684	7.1184	1.864	46.42/15.57	0.093	30.85
6.	25000	1350	490	0.4019	7.1519	1.864	44.90/16.27	0.0677	28.63
7.	30000	1300	500	0.4266	7.1766	1.865	43.35/16.65	0.0494	26.70
8.	35000	1250	530	0.4428	7.1928	1.865	41.72/17.67	0.0323	24.05
9.	40000	1200	540	0.4544	7.2044	1.866	40.15/18.05	0.0232	22.10
10.	45000	1150	540	0.4627	7.2127	1.866	38.49/18.04	0.0166	20.45
11.	50000	1100	520	0.4697	7.2197	1.867	36.80/17.38	0.0140	19.42
12.	55000	1050	510	0.4751	7.2251	1.867	35.25/17.08	0.0108	18.17
13.	60000	1000	490	0.4793	7.2293	1.867	33.50/16.40	0.0084	17.10
14.	65000	900	410	0.4830	7.2330	1.868	30.17/13.72	0.0074	16.45
15.	70000	750	300	0.48566	7.2356	1.868	25.13/10.13	0.005	15.00

ME-1974-M-SEH-STU